

Bachelor Thesis

**Effectiveness of glacial and fluvial erosion in granitic,
volcanic, and sedimentary drainage basins in Wyoming**

Lukas Malle

Department of Geology and Geophysics, University of Wyoming, Laramie Wyoming

(May 2019)

Content

1. Abstract	3
2. Introduction	4
3. Study Area	5
3.1. Climatic Overview	5
3.2. Geography	7
3.2.1. Wind River Range	7
3.2.2. Wyoming Range	8
3.2.3. Absaroka Range	8
3.4. Geology	10
3.4.1. Absaroka Range	10
3.4.2. Wyoming Range	11
3.4.3. Wind River Range	11
3.5. Glacial History	11
4. Data and Methods	13
4.1. Climatic data	14
4.2. Geologic data	15
4.3. Morphometric measures	15
4.4. Stream network Strahler	18
4.5. Channel Steepness and Channel-reach morphology	19
5. Results	21
5.1. Geology	21
5.2. MATLAB Analysis	23
5.2.1. Hypsometric curves	23
5.2.2. Longitudinal River Profiles	25
5.3. GIS Analysis	28
5.3.1. Slope	28
5.3.2. Channel – reach morphology	29
6. Discussion	31
6.1. Glacial valley morphology related to rock strength and lithology	32
6.2. Valley stream morphology based on stream-reach types	35
7. Conclusion	39
8. References	40

1. Abstract

Glaciers and rivers are the main driving forces in shaping valleys in alpine landscapes. In this study, three watersheds in north-western Wyoming with different lithologies were examined for spatial differences in the morphological valley development affected by quaternary glaciation. To prove the hypothesis that watersheds with more resistant igneous bedrock develop steeper sided, narrower valleys, morphometric analyses on high-resolution digital elevation models were implemented in the Absaroka Range (volcanic rocks), in the Wind River Range (granitic rocks) and in the Wyoming Range (sedimentary rocks). The study area has a rather uniform climatic and glacial history that makes it an ideal location to study the effects of glacial erosion and river incision on the shaping of topography. The results of the analysis demonstrate that in the longitudinal river profiles, the resistant granite has a stair-stepped profile that differs from the volcanic and sedimentary basins that have much smoother profiles because of their less resistant bedrock. To get a better understanding of the impact of glacial profiles development on the modern rivers in the drainage system of the three watersheds, stream-reach types (colluvial, cascade, step-pool, plane-bed, pool-riffle) were classified based on a channel steepness index derived from the observed morphology. While more resistant bedrock has the steepest stream sections, it also has the greatest proportion of low gradient pool-riffle streams because of low gradient sections of tributary valleys at some of the highest elevations.

2. Introduction

Glaciers played an important role in shaping the alpine landscapes in the last two million years, in combination with sedimentation and tectonism that began in Late Cretaceous time (Love, 1977). In the western United States, multiple glacial advances have shaped the watershed morphology in modern landscapes (Pierce, 2003). Glaciers shape landscapes very differently than those in which rivers are the main erosive agent, and glacial erosion rates far exceed fluvial erosion rates (Anderson et al., 2006). Bedrock strength characteristics from different lithologies are also an important factor in controlling morphology of those glacial valleys (Brook et al., 2004). Where bedrock is resistant, troughs are deep and narrow, and wider and shallower where it is less resistant (Matthes, 1930). Further, glaciers are generating steps instantly downvalley of tributary junctions (see fig.5), leaving tributary valleys hanging. Thus, the increase in ice discharge below such tributary junctions, results in forming those steps and overdeepenings in the trunk valleys (MacGregor et al., 2000).

Nowadays most of the glaciers melted away and as a consequence, the modern stream system needs to adapt to the shaped valley landscape profiles left by glaciers.

The Absaroka Range (volcanic rocks), the Wyoming Range (sedimentary rocks), and the Wind River Range (granitic rocks), all experienced those glacial episodes and makes them an ideal natural laboratory to study the influence of lithology in the morphological landscape shaping. On the one side, I will present the glacial valley development of all three lithologies through morphometric analysis, and, on the other side, I will present an examination of the post-glacial drainage systems based on their

stream-reach types. Indeed, those circumstances allow me to define several hypotheses to explain the potential different landscape characteristics:

1. More resistant bedrock, like the granite in the Wind River Range, should develop steeper sided, narrower valleys with a more stair-stepped profile.
2. Volcanic bedrock should be classified as less resistant bedrock, showing a smoother profile than the granite but still showing steeper sided and less wide valley walls than the sedimentary bedrock.
3. The stream-reach types in the drainage system should show a higher frequency of steeper stream-reach types (colluvial) in resistant bedrock and flatter stream-reach types (pool-riffle) in less resistant bedrock.

3. Study Area

3.1. Climatic Overview

The climate in the selected study areas in all three lithologies is fairly similar because they are not so far apart, so a good comparison between all three watersheds can be made (fig. 1). Topographic asymmetry can result in receiving appreciably greater amounts precipitation and can inform a conceptional model of range evolution (Foster et al., 2010). Hence, rates of precipitation increase with elevation and pacific westerly winds occurred both at the last glacial maximum (LGM) but are still dominating today. That's why modern patterns of precipitation are broadly comparable to those at the LGM (Love et al., 2003, p.95; Meyer et al., 2004). According to Foster et al. (2010), that the total catchment precipitation is important to investigate because the majority

of snow that fell on supraglacial hillslopes is still contributing to glacial accumulation following transport downslope by avalanching.

Insolation (incoming solar radiation) is also an important factor in how topographic shading influences the distribution of glaciers during the summer melt season, which results in that stream flow is dominated by snowmelt during the summer month (Foster et al., 2010).

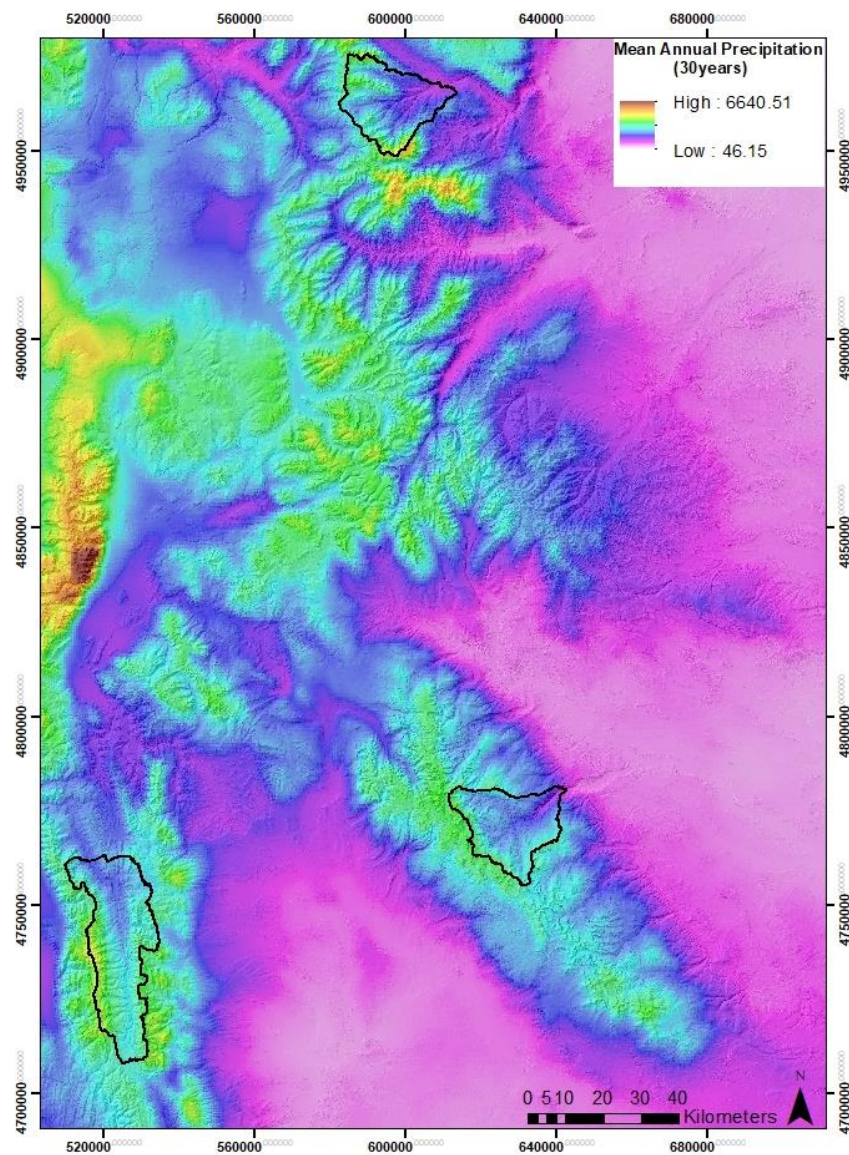


Figure 1: Climatic Overview of the study area. All watersheds of the three lithologies are marked with a black border shape around them. They all show similar climatic conditions.

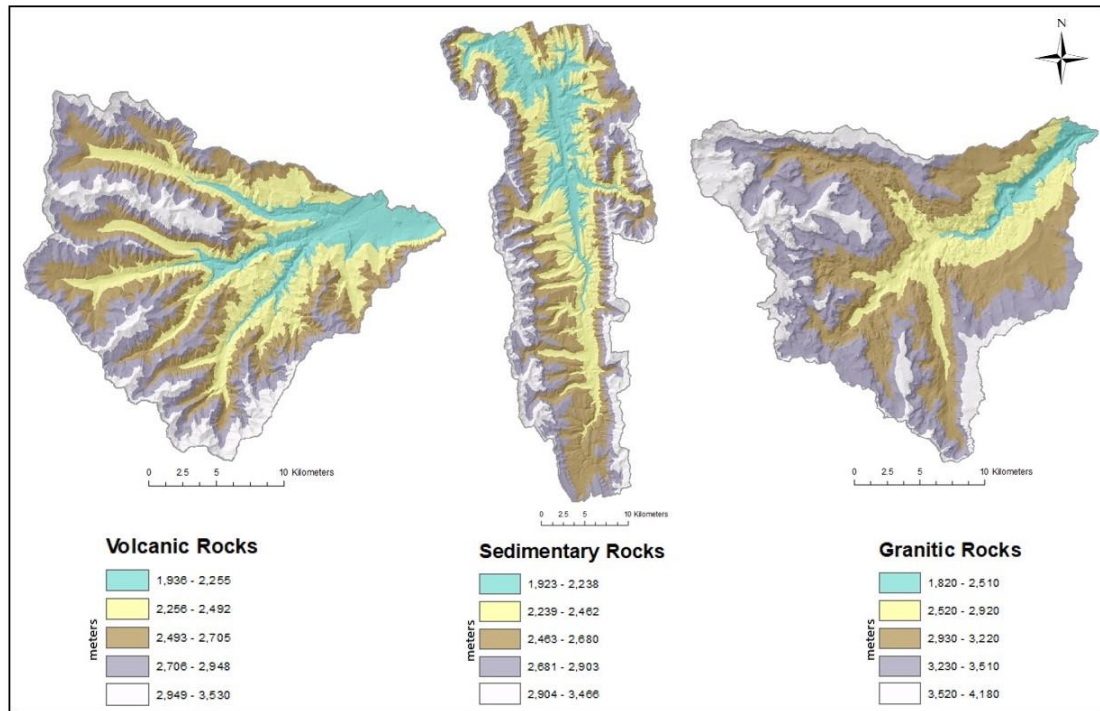


Figure 2: Outline of the three watersheds with their different elevations

3.2. Geography

3.2.1. Wind River Range

The Wind River Mountains are eroded from a northwest-southeast-trending anticline (Branson et al., 1941), and are located in the Middle Rocky Mountains of west-central Wyoming about 100 miles south-east of the Yellowstone Park (fig. 3). With a length of 150 miles and a width of about 40 miles the range separates the Green River Basin on the west side and the Wind River Basin on the east. The range rises above a general level of about 1500 m on the east to about 2100 m in the west, whereas the maximum elevation in the Range is the Gannett Peak with 4200 m, which is also the highest mountain in Wyoming. The actual study area with the selected watershed for the morphometric analysis, with a size of about 460 km², is placed on the north-east of the

range between Crow Mountain and Bull Ridge. The tributaries of the drainage basin coalesce to the west of the range into Bull Lake Creek that flows directly into the Bull Lake, located on the eastern side of the Wind River Range.

3.2.2. Wyoming Range

The north-south trending Wyoming range is located in the Rocky Mountains in western Wyoming on the eastern boarder of Idaho. With Wyoming Peak as its highest peak, which stands at around 3,400 meters above sea-level, it is the range with the lowest average elevation. As the range almost runs parallel to the boarder of Idaho it also runs along the Highway 89 and towns like Afton are located on the western base of the ridge. On the eastern side of the ridge, the river drains into the Green River Basin, which separates it from the Wind River Range. However, there is the Greys River draining from south to north of the where it later runs into the Palisades Reservoir in Idaho. It is also the main river in the selected drainage basin where all tributaries from the selected watershed drain into and has an area of 560 km², slightly bigger than the other drainage basins.

3.2.3. Absaroka Range

The Absaroka Range is located also in the Middle Rocky Mountains in west-central Wyoming. It stretches about 150 miles north-south across the Montana-Wyoming border and with 75 miles at its widest, the range forms the eastern boundary of Yellowstone National Park in Wyoming and continues north along the eastern margin of the Yellowstone River valley in Montana. On the eastern side the Bighorn Basin is adjoining the Absaroka Range. The North Fork Shoshone River and the South Fork Shoshone

River are two major rivers draining to the eastern side of the range into the Bighorn Basin and congregate into the Buffalo Bull Reservoir, west of Cody. The highest peak in the range is Francis Peak in Wyoming, with an elevation of about 4000 m.

The selected watershed in the Absaroka Range has a size of around 460 km² and is located northeast of Yellowstone Lake in the North Absaroka Range. The tributaries of the drainage basin drain together into Crandall Creek which later joins the Clarks Fork Yellowstone River.

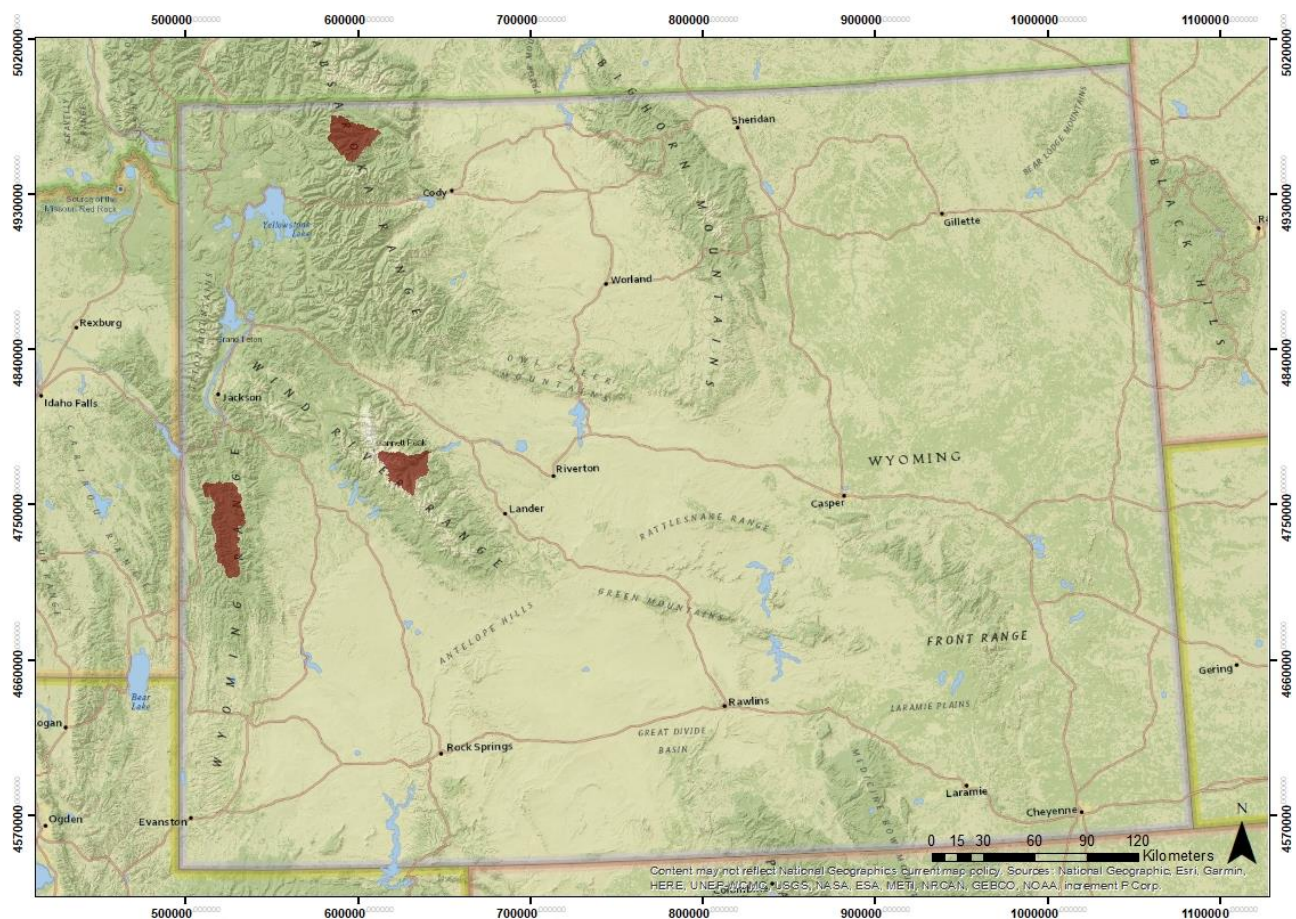


Figure 3: Geographic Overview of the study area. The different watersheds are marked in red.

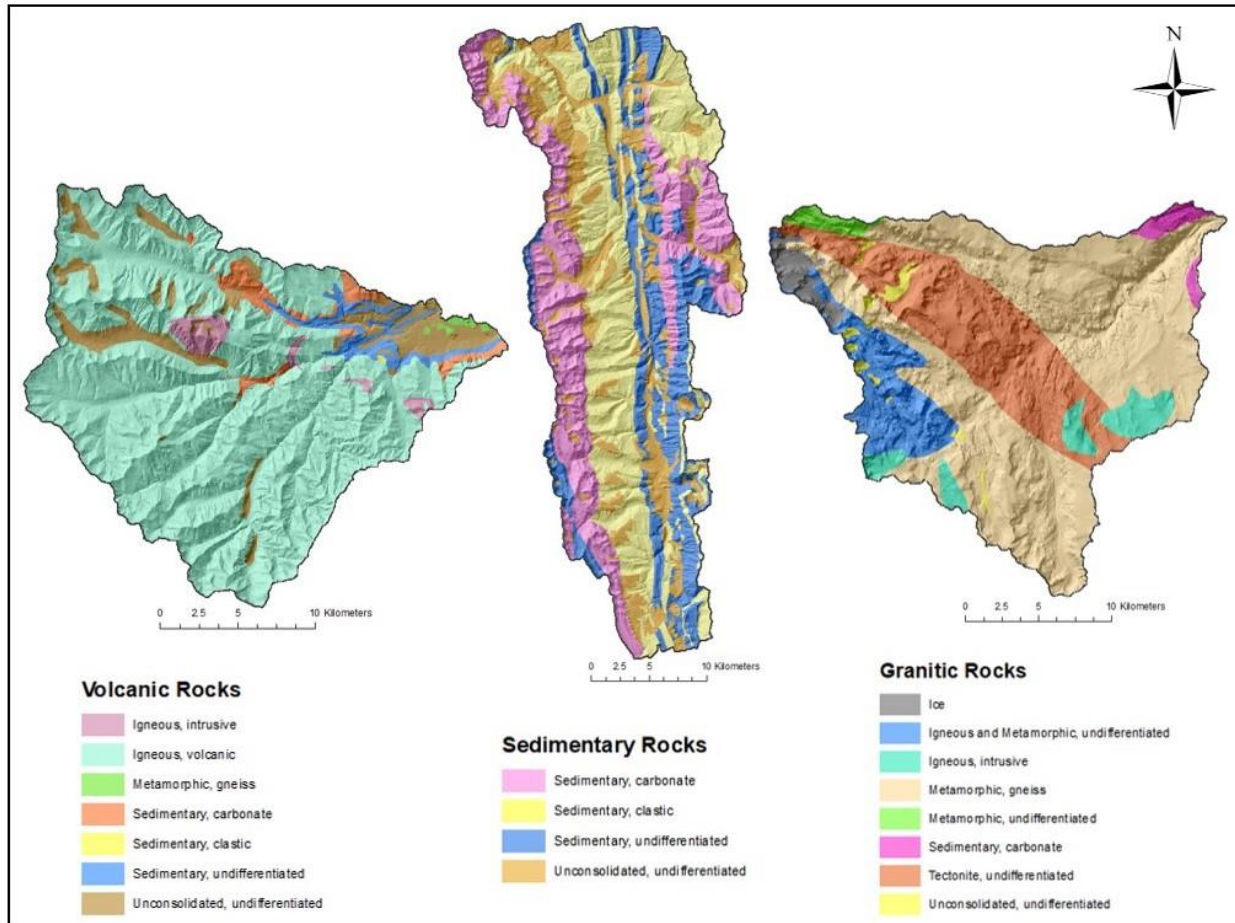


Figure 4: Geologic structure of the three drainage basins.

3.4. Geology

3.4.1. Absaroka Range

During the Eocene epoch, extensive outpourings of predominantly andesitic lava flows, accompanied by a great volume of volcanic breccia, engulfed a region that extended from near Bozeman, Montana to about 150 miles southeastward into Wyoming (Chadwick, 1970). The Absaroka Mountain Range is the remnant of this large volcanic field that was active in the Middle Eocene for about 10 million years. There were twelve volcanic centers generated volcanos that rose up to 3,000 meters above the valley floors. The northern Absaroka Mountains are predominately composed of Tertiary basaltic volcanic rocks. The

rocks deposited from these volcanos comprise now the Absaroka Volcanic Supergroup (Blackstone, 1986). The high peaks of the range were sculpted by several glacial cycles, and moraine and terrace deposits are common along the streams draining these mountains.

3.4.2. Wyoming Range

The selected study area in the drainage basin with the Greys River in the Wyoming Range formed during the Sevier Orogeny, a fold and thrust belt that was active approximately 155-50 million years ago (Wyoming Geological Survey, 2019). The geology consists of thrust sheets of Mesozoic and Paleozoic sedimentary rocks.

3.4.3. Wind River Range

The core of the Wind River Range consists of pre-Cambrian granodiorite and metamorphics on which the higher parts of the range and the glaciated peaks are developed on. On the northeastern side Paleozoic sediments form foothills and Mesozoic sediments underlie hogbacks and valleys paralleling the axis of the range (Branson et al., 1941).

3.5. Glacial History

Love (1977) describes four major different glacial events that affected the study watersheds. The first glaciation event took place somewhat more than two million years ago in the Jackson Hole area and on the adjacent uplands. It is referred informally as the “ghost glaciation”, because it has not been named or recognized in publications on the area. The second glaciation in this area is much more clearly documented than the first one. Even though the exact age is not known, it is younger than 1.9 million years (Love,

1977). The ice shield had sources in Yellowstone National Park and in the Absaroka, Teton, Gros Ventre, and Wind River Range and the ice streams coalesced in Jackson Hole. Here the ice had a thickness of about 3000 feet and flowed from there southward along the Snake River Valley, through the Snake River Canyon and into Idaho.

The third major glaciation, called the Bull Lake event, was only half as extensive in Jackson Hole as the second. Obsidian hydration dating shows that this glaciation occurred between 130,000 and 155,000 years ago (Pierce et al., 1976). The fourth and last glaciation, called the Pinedale event, was the smallest of the four glaciations with several ice advances that occurred between the last 35,000 and 9,000 years ago (Love, 1977).

Several generations of glaciers produced magnificent alpine scenery in the Wind River Range and during those periods the topography governed the glaciation to a great extent. Hence Holmes (1955) argues that's why the axial portion of the range consists of sharp peaks and ridges separated by short, structurally controlled valleys. Each glacial episode produced a characteristic complex of glacial and glaciofluvial deposits which are still very well preserved in and around the Wind River Range. A reason for that is that because most of the materials in the range are largely crystalline rocks highly resistant to weathering. Further the original volume of the deposits was very large, and many were laid down on flat erosional surfaces or wide valley bottoms where post depositional erosion has not been great. Hence both the moraines and outwash facies of the several glacial advances are still preserved in this area. The glacial terraces retain their topographic and lithologic identities for scores of miles down the main streams even though their height is not uniform. In the first few miles downstream, near the moraines,

stream gradients are steep, the bedrock is not homogenous, and trenching of the valleys below the outwash has been deep (fig.5) (Holmes, 1955).

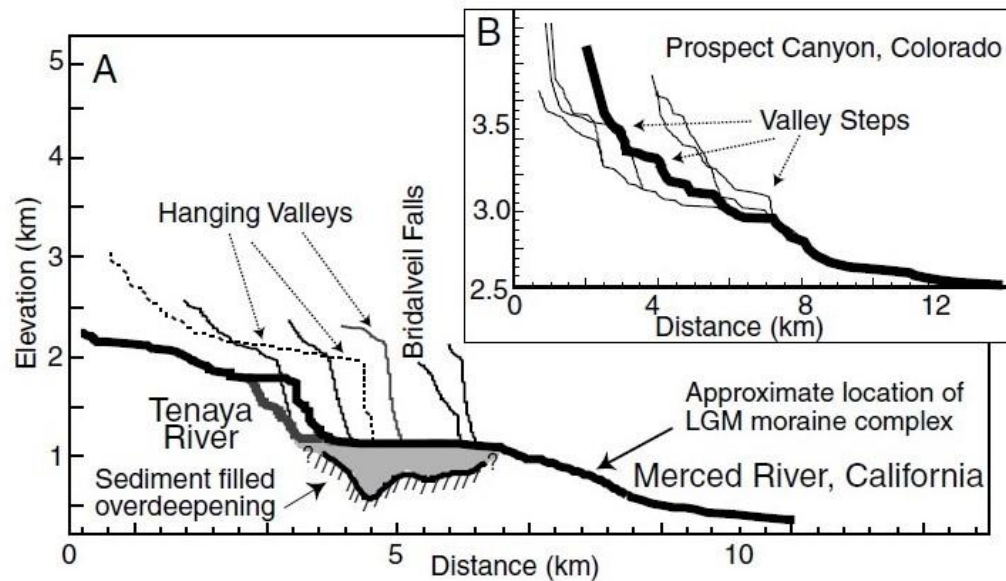


Figure 5: Setup of hanging valleys and overdeepenings (reproduced from Holmes, 1955).

4. Data and Methods

The geomorphometric analysis of the river drainage areas in the Wind River Range, the Wyoming Range and the Absaroka Range were implemented in MATLAB and with the GIS program ArcMap. The analysis is based on the 1/3rd arc-second (approximately 10 m resolution) Digital Elevation Model (DEM), out of the tiled collection of the 3D Elevation Program (3DEP), provided by the U.S. Geological Survey (USGS) from 'The National Map'. The 3D Elevation Program is collecting 3D elevation data in the form of light detection and ranging (lidar) data across the United States for high resolution mapping of the land surface, useful for multiple applications (Sugarbaker et al., 2017). For this analysis multiple extents of 1/3 arc-second 2013 1 x 1-degree raster datasets were

merged with the mosaic tool in the Data Management Toolbox into a single raster dataset to cover the selected study area for the final calculations.

4.1. Climatic data

The climatic data for the mean annual precipitation for the last 30 years is obtained from an 800 m resolution map generated by the PRISM (Parameter elevation Regressions on Independent Slopes Model) that is based on a 30 year (1981-2010) average precipitation dataset. In general PRISM collects point climate measures from a network of weather stations and creates continuous grids of temperature and precipitation interfacing with a landscape DEM, using a linear climate elevation regression function which reflects the strong bond between the climate and topography (Foster et al., 2008). According to Daly et al. (2002, 2008), the model is using a moving window algorithm, creating a unique linear regression function for each cell in between the grid, whereas precipitation values are tied to the grid cell elevation. The nearest 40 weather stations are examining the measures of precipitation data for the regression function, and then assign a weighting by reading the distance between and the physiographic similarity, based from each station, of the weather station and grid cell in question. The predicted precipitation values are then compared to measured values and results of statistical uncertainty tests, to assess the validity of the model outputs (Daly et al., 2002, 2008)

However, neither a high-resolution PRISM output map nor detailed precipitation data for each watershed location is the main aim of this study. To make sure to get a good comparison between all three lithological basins, it was simply important for the selection of the drainage basins, to make sure they are all situated in almost the same climatic areas showing similar precipitation data.

4.2. Geologic data

The geologic map was also provided by the USGS from the State Geologic Map Compilation (SGMC) Geodatabase of the Conterminous United States. It represents a seamless, spatial database of 48 state geologic maps that range in scales from 1: 50,000 to 1: 1,000,000. Though, because geologic units have not been standardized, the SGMC is not a truly integrated geologic map database. Hence, the geologic data contained in the geologic map of each state have been standardized to allow spatial analyses of lithology, age, and stratigraphy at a national scale (Horton et al., 2017).

In this study the SGMC was cropped to each watershed to make sure that each watershed conforms to the expected lithology (volcanic, sedimentary, granitic) to get reliable data results out of the analyses (fig 4).

4.3. Morphometric measures

The focus of the geomorphometry in the analysis was the extraction of measures (land surface parameters) and spatial features (land surface objects) from the digital topography in the DEM. Land surface objects are discrete surface features like watershed boundaries or drainage networks, whereas land surface parameters are descriptive measures of a surface form like slope or aspect and they can also be differenced in primary and secondary parameters (Wilson, 2011).

As Olaya (2009) noted, primary land surface parameters are derived directly from the DEMs without any additional inputs or further knowledge of the area represented. He also distinguished the primary land surface parameters into local and regional parameters, where local parameters are attributes like slope or aspect that are calculated by moving a three-by-three window across a grid and calculating land surface parameters

for the central cell in the three-by-three window. Wilson (2018) remarks that regional land surface parameters are by contrast mainly concerned with the climatic, geomorphic and hydrological parameters. These geomorphic and hydrological parameters focus on the movement of water and sediment and rely on an accurately delineation of watersheds. In this analysis regional parameters like flow-path length and statistical measures that summarize the elevation and slope values down-, and upslope of each grid cell, were used. Many of those parameters are derived from calculating the flow direction grid by using the deterministic eight node algorithm (D8), that permits flow to one of eight neighbors based on the direction of steepest descents on a square-grid surface model (O'Callaghan & Mark, 1984). A distinction is drawn between single- and multiple-flow direction algorithms. In the single – flow direction, that was used in this analysis, the flow is directed to just one downslope or neighboring cell including the D8 algorithm. The multiple flow-direction algorithms in contrast, can direct flow to two or more downslope or neighboring cells Wilson (2018).

Based on this analysis, the accumulated flow as the accumulated weight of all cells flowing into each downslope cell in the output raster was calculated with the Flow Accumulation tool in the Hydrology toolset. If there is no weight raster provided, a weight of 1 is applied to each cell and the value of cells in the output raster is the number of cells that flow into each cell. Cells with a high flow accumulation are considered as areas with concentrated flow and could be used to identify stream channels whereas cells with a flow accumulation of 0 are considered as local topographic highs and could be used to identify ridges (Tarboton, 1991).

DEMs from each study area location, generated in ArcMap, were then implemented in MATLAB for further calculations. For this the Topo Toolbox, a MATLAB software for the analysis of DEMs (Schwanghart, 2013), was used. A hypsometric curve was produced for every watershed to compare the horizontal cross-sectional areas of the landmasses with respect to elevation. The use of absolute units for the analysis of the form quality of erosional topography is unsatisfactory because areas of different size and relief cannot be compared, and the slope of the curve depends on the arbitrary selection of scales (Strahler, 1952). That's why in my analysis for the hypsometric curves uses dimensionless parameters, independent of absolute scale of the topographic features. To reach this, Strahler (1952) describes, that there are two ratios involved: (1) the ratio of area between the contour and the upper perimeter (Area a) to the total drainage basin area (Area A), depicted on the abscissa (X-Axis) on the coordinate system; (2) the ratio of height of contour above base (h) to the total height of basin (H), represented by values of the ordinate. The resulting hypsometric curve (Fig.6) allows to compare forms of different basins of different sizes and elevations. It expresses in which the volume lying beneath the ground surface is distributed from base to top and the curve must always originate in the upper left-hand corner of the square ($x=0$, $y=1$) and reach the lower right-hand corner ($x=1$, $y=0$).

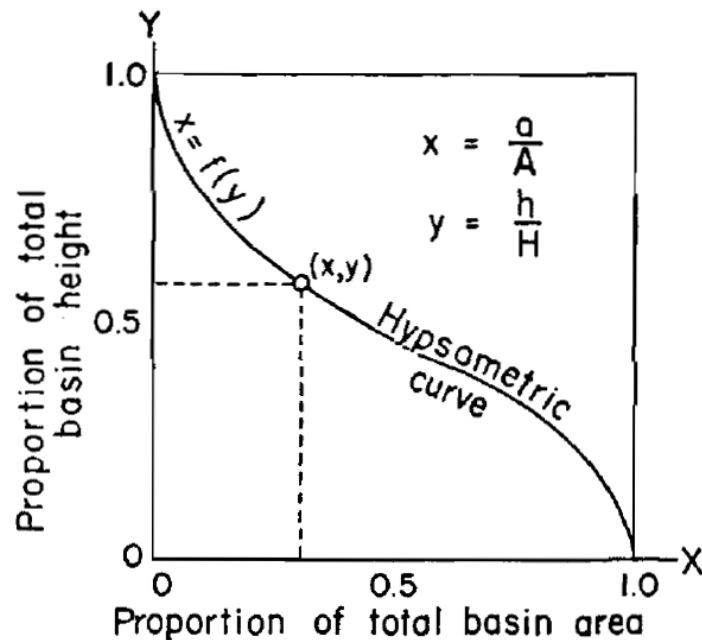


Figure 6: The Percentage Hypsometric Curve (reproduced from Strahler, 1952)

4.4. Stream network Strahler

In addition to the geomorphometric analysis of the watersheds, I am also evaluating how the stream and river network has developed in these different watersheds (fig.11). One such analysis, fundamental for the later topographic slope gradient calculations of the stream channels, was the Strahler Stream Order classification to identify different stream types based on their numbers of tributaries (fig. 7). In this method all links without any tributaries are referred to as first order and the stream order increases when streams of the same order intersect. For example, when two first- order channels join, a channel of Order 2 is formed and where two of Order 2 join, a segment of Order 3 is formed, and so forth (Strahler, 1957).

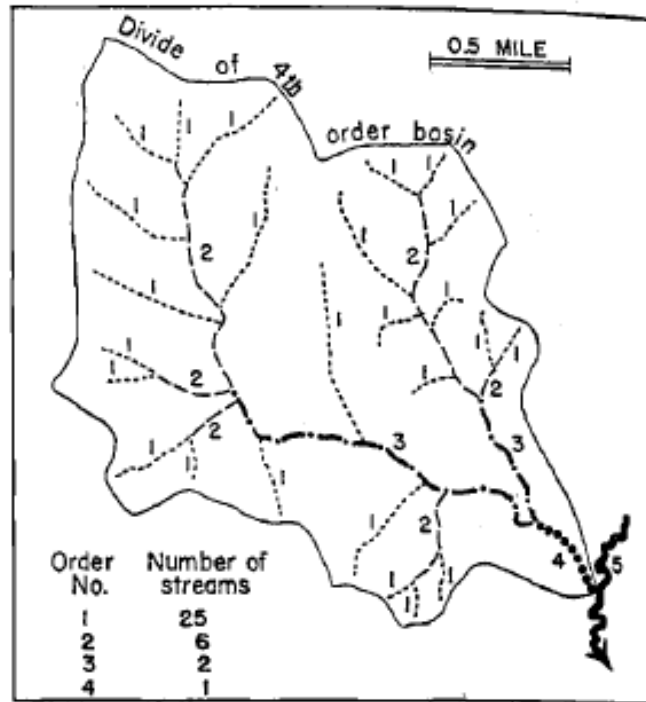


Figure 7: Method of designating stream order (reproduced from Strahler, 1954, p. 344)

4.5. Channel Steepness and Channel-reach morphology

Another relevant analysis was implementing the slope steepness with ArcMap, where the maximum rate of change in value from a cell to its neighbors is calculated. The maximum change in elevation over distance between the cell and all eight neighbors then identifies the steepest downhill descent from that cell (Burrough and McDonnel, 1998). Hence, this is important because the channel steepness of the stream network derives from the slope calculation. Once the drainage channel network is combined with the slope data, a mean channel steepness downstream is the result. With a simple reclassification of the results, stream reach types after Montgomery and Buffington can be generated.

According to Frissell et al. (1989) channel units, stream reaches, and valley segments are three partitioned subdivisions of the drainage network within watersheds.

This represents the largest physical subdivisions that can be directly altered by human activities and exerts a powerful influence of the distribution and abundance of animals and aquatic plants by governing characteristics of surface and shallow subsurface water flow and also the capacity of streams to transform organic matter and store sediment (Bisson et al., 2017)

In this study the focus is on the channel-reach morphology which Montgomery and Buffington (1997) classified into seven distinct reach types (fig.8): colluvial, bedrock, and five alluvial channel-reach types (cascade, step pool, plane bed, pool riffle, and dune ripple). Steep alluvial channels (cascade and step pool) show a high sediment transport capacity ratio, whereas low gradient alluvial channels (pool riffle and dune ripple) have lower transport capacity to supply ratios and thus exhibit a significantly response to changes in sediment supply and discharge (Montgomery and Buffington, 1997)

However, in the analysis a reclassification of Montgomery and Buffington's (1997) stream-reach types was realized, whereby colluvial segments occur in steeper areas than 16.7 degrees, cascade can be found between 5.7 and 16.7 degrees, step – pools between 1.72 and 5.7 degrees, plane – beds between 0.6 and 1.72 degrees and pool – riffles between 0 and 0.6 degrees slope (fig.14).

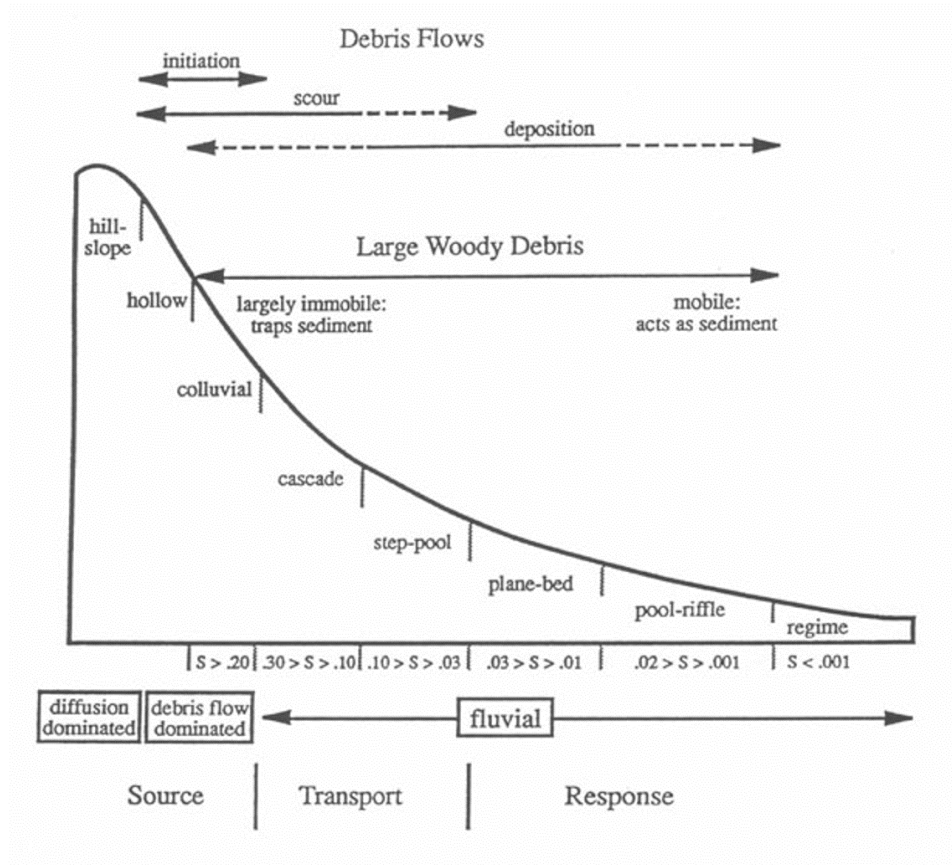


Figure 8: Classification of an idealized long profile from hillslopes and unchanneled hollows downslope through the channel network showing the general distribution of alluvia channel types and controls on channel processes in mountain drainage basins (Montgomery and Buffington, 1997).

5. Results

The goal of this study is to show that different lithologies act differently in shaping watershed morphology in landscapes affected by Quaternary glaciation. To prove this, several analyses were implemented as already described in detail in the Data and Method section. In this section the outcome of those analyses will be presented.

5.1. Geology

It was not possible to do complex geologic field work in all three-different selected study areas, but USGS digital geologic maps cropped to the drainage basins of the

different lithologies provide a good overall description of the geology (fig.4). To get a better comparison between the three different lithologies in the study areas it was taken heed to only select the study areas with mostly monotonous bedrock and a not too big variety in the geologic setting or too much unconsolidated material covered. This is important because the focus was on how the volcanic, sedimentary, and granitic bedrock differ in the topographic landscape developing that is shaped by rivers and glaciers.

The volcanic watershed (Crandall Creek) consists mostly of igneous volcanic bedrock, and some little spots of igneous intrusive bedrock throughout the drainage basin. Though in the very eastern part of the basin at lower elevations, carbonate and clastic sedimentary bedrock is increasing. Unconsolidated material shows up at some patches on the base of steeper slopes as a result of erosional processes.

The Greys River watershed is mostly composed out of carbonate and clastic sedimentary bedrock whereas the eastern part of the basin is intervened with undifferentiated sedimentary rocks. Unconsolidated material is spread over the whole basin along some valleys.

The granitic drainage basin (Bull Lake Creek) is mostly build out of metamorphic gneisses. The middle area of the watershed is traversed by an undifferentiated Tectonite belt. Undifferentiated igneous and Metamorphic bedrock occur on the western part of the basin in a small amount, where the northwestern part is covered by a small glacier. Furthermore, some intrusive igneous bedrock appears in smaller spots on the southern side of the basin. Importantly, most of the metamorphic rocks in the Wind River Range are considered granitic gneiss, originally formed as granitic plutons during the Archean

and exposed following the Laramide Orogeny (Frost et al., 2000). Therefore, the rocks of the Wind River Range are primarily plutonic (granitic) in origin, in contrast to the extrusive volcanic and sedimentary rocks of the other basins.

5.2. MATLAB Analysis

5.2.1. Hypsometric curves

The hypsometric curves and their integrals for the lithological domains of all three study areas show significant differences between the different lithologies (fig. 9). The local base levels are almost the same, however the granitic basin shows with almost 4000 m the highest elevations whereas the volcanic basin shows a maximum elevation of about 3500 m and the sedimentary basin has the lowest maximum elevation with about 3000 m. While this difference may be related to tectonic history, in addition to lithology, most of the modern topography in the western U.S. has been shaped during widespread river incision in the late Cenozoic (Anderson et al., 2006). Thus, the difference in the highest elevations in each range likely owe in large part to the differences in erosional resistance due to lithology. In general, all three lithological hypsometric curves feature a decrease of area with an increasing surface elevation where the hypsometric maximum is located in the lower elevations.

The volcanic curve starts at an elevation of about 3500 m and gently loses height till 2500 m with a low increase of area. From 2500 m till the base there are less elevation changes, but a higher area increase is the result. Further, the mean elevation in the basin is about 2600 m (Table 1). The curve looks also similar then the sedimentary basin,

though the “tail” of the curve shows more area at high elevations compared to the sedimentary watershed.

The Sedimentary basin shows the smallest hypsometric integral of all three lithologies. The hypsometric curve starts at an elevation of about 3000m and displays a very rapid elevation change till about 2500 m. From there the area is increasing constantly till the base. With a mean elevation of 2557m (Table 1) it is, similar than the volcanic watershed, closer to the minimum elevation, which indicates that the highest elevation topography occupies a small area relative to the whole basin, though the “tail” of the curve or the second hump in the distribution is also closer to the highest elevations but less than the volcanic basin.

The granitic curve shows in contrast the highest hypsometric integral. The curve starts at around 4000 m and only depicts a small elevation change but a constant area increase till about 2500 m where it reaches the hypsometric maximum and then decreases straight to the base. Moreover, the mean elevation with about 1820 m, is about halfway between the minimum and maximum elevation, which indicates that the basin has more area at a higher relative elevation. What make the curve almost look like a classic normal distribution (“bell curve”).

Table 1: Statistical overview of the elevations in all three watersheds.

Elevation	Volcanic Rocks	Sedimentary Rocks	Granitic Rocks
minimum	1936 m	1923.03 m	1820.12 m
maximum	3529.7 m	3466.24 m	4179.06 m
mean	2611 m	2557.21 m	3184.42 m

5.2.2. Longitudinal River Profiles

In total the graphs with the drainage area versus the distance upstream, show distinct differences that may be related to the contrasting lithology between those three study areas. In general, the graphs of the different lithologies show a close relationship between the drainage area and the stream length. The longer the stream flow distance the bigger the drainage area gets. Furthermore, the steepness of the river profile decreases with the flow length of the stream.

The volcanic basin shows that the drainage area decreases very rapidly at 5 km upstream where a major tributary enters, and then constantly decreases upstream towards its headwaters (fig.9 A). The longitudinal river profile increases elevation-wise very constantly with very tiny elevation changes almost not visible. Upstream at higher elevation most tributaries drain the main river with the highest order whereas in lower elevation the density of draining tributaries decreases (fig.9 D). Most of the tributaries show steep channel profiles from the main stem channel to their headwaters.

The sedimentary basin displays an almost constant drainage area decrease with a longer stream flow length in uphill direction, indicating a lack of large tributaries entering this basin (fig. 9 B). The basin has also the biggest drainage area size and longest stream length of all lithologies. The longitudinal river profile is almost perfectly graded with a smooth elevation profile throughout the basin elevation (fig.9 E). Smaller tributaries enter consistently downstream through the basin and exhibit similarly steep profiles from the main channel to the headwaters.

The granitic basin shows again a very different behavior of the river profile than the sedimentary and volcanic basins. The drainage area decreases at the beginning very

linearly until about 2km upstream where it loses quickly a lot of its size upstream from a major tributary, and then decreases almost linearly till the river origin upstream (fig.9 C). The longitudinal river profile displays the biggest difference with its stair stepped profile what is very characteristic for resistant granitic rocks. In general, steps in the profile occur at locations where tributary glaciers would have entered the main valley. In the higher elevations more, tributaries at a higher frequency drain into the main river than in the lower elevations (fig.9 F). Another striking difference in the granitic profile are the low gradient sections of tributary valleys at some of the highest elevations (fig. 14). These features likely represent hanging valleys and cirques that are much rarer in the Wyoming and Absaroka Ranges.

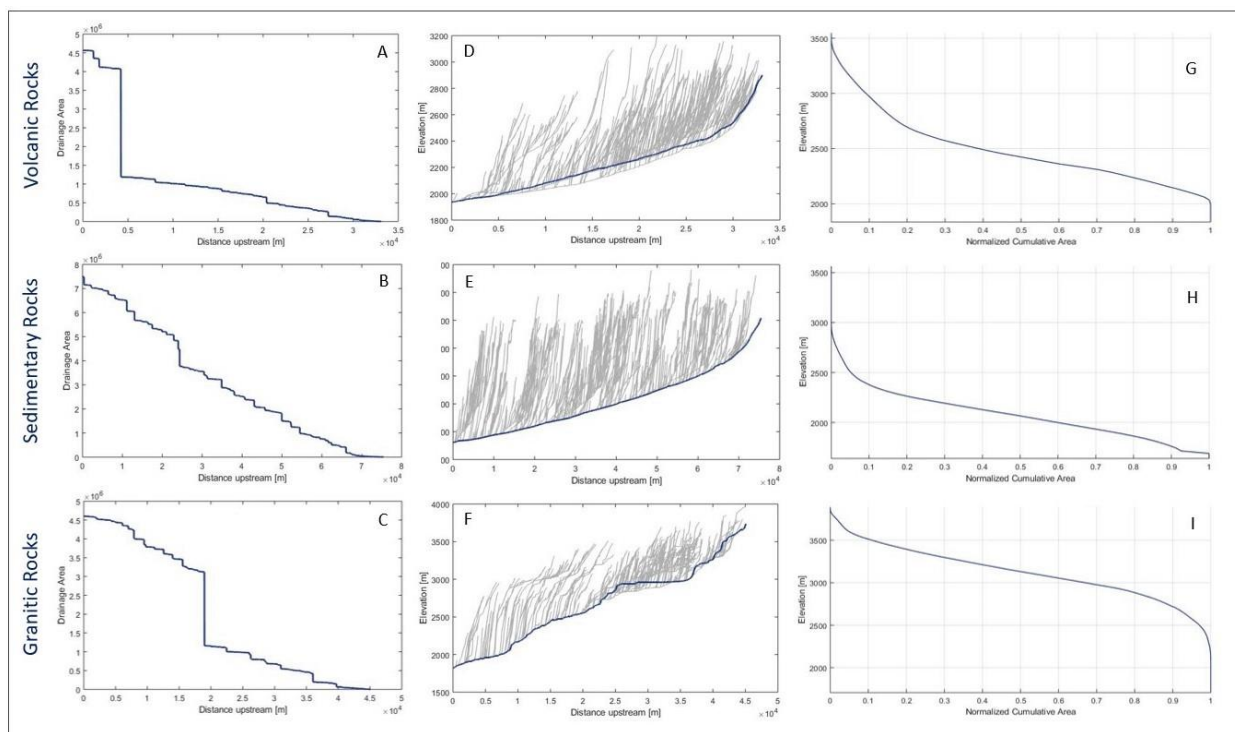


Figure 9: Hypsometric Curves and longitudinal river profiles of each lithological location. Volcanic Rocks (A-G), Sedimentary Rocks (B-H) and Granitic Rocks (C-I).

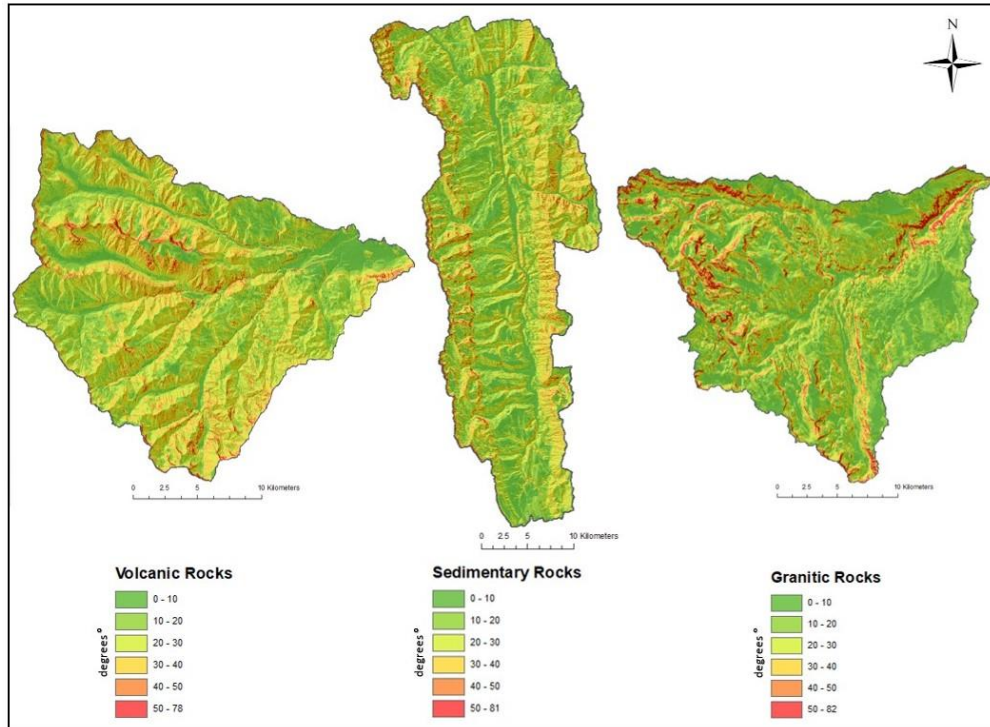


Figure 10: Overview of the topographic steepness gradient into the slope map. Green areas show flatter areas, whereas the red parts show the steepest parts of the watersheds.

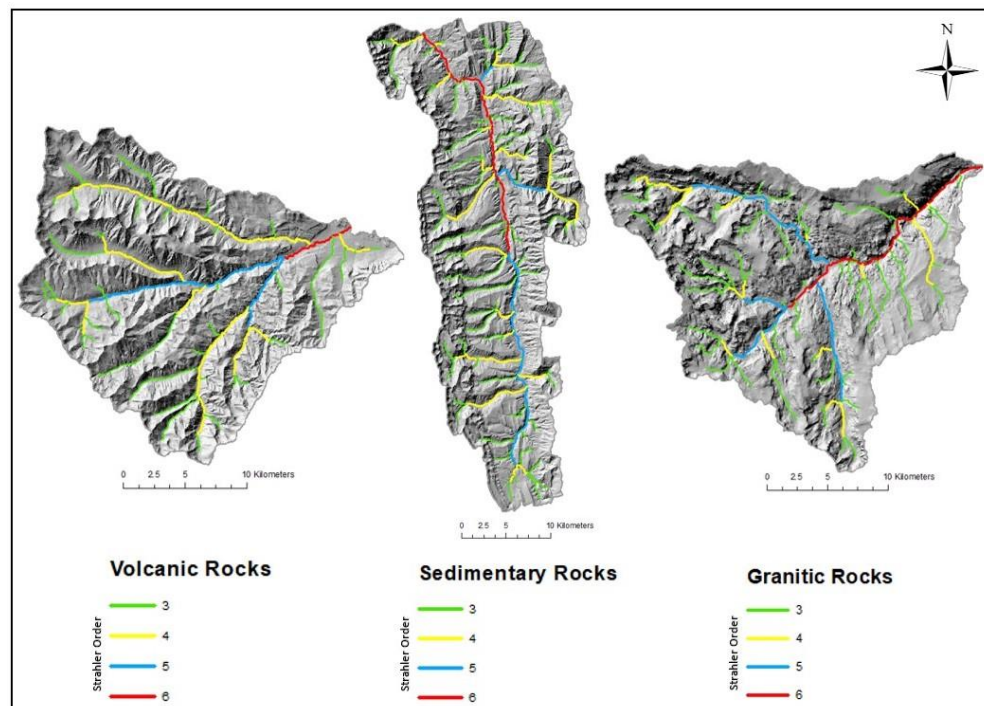


Figure 11: Strahler Order from 3 to 6 in all three lithological watersheds.

5.3. GIS Analysis

5.3.1. Slope

The slope maps show in all 3 different lithologies that the topographic steepness gradient is high at the steepest parts of the mountain ridges at higher elevations, labeled with a red color (fig.10). Flatter areas with less slope degrees are marked greenish. However, it is hard to visualize those differences between the lithologies in the graphs. That's why with a reclassification the steepness degrees were modified to pixels of slope to see how many pixels at every elevation are counted. Then it is possible to tell how many percent of the steepest parts of the drainage basin occur in different elevations. Six classes were used to visualize the results of the topographic steepness gradient classified every 10 degrees from 0 to 50 degrees and everything what is above.

The volcanic basin shows with 78 degrees slope the least steep parts, though the overall percentage of slopes steeper than 40 degrees has a higher frequency than the sedimentary watershed, which has a higher maximum steepness with 81 degrees but has less abundance for higher steepness's showing by the more greenish slopes than red parts in the map (fig.10). The granitic basin displays with 82 degrees the highest overall steepness and also the highest frequency of higher elevations with a lot of red areas on the map. Hence, it also shows a big amount of low elevations from 0 to 10 degrees, what is not as good visible in the slope map, but it is filters out of a statistical analysis of the slope.

5.3.2. Channel – reach morphology

To get a better overview about how the river drainage network interacts with the topography, the topographic steepness gradient, derived from the slope map, was used to get a better depiction for all three study areas. An important implication of differences in valley profiles and channel steepness in the three different drainage basins are the different stream - reach types that Montgomery and Buffington (1997) describe for differences in channel gradient. For the three watersheds discussed in this paper the focus is on following stream types starting from lower elevations with flatter areas and ascending to higher elevations with steeper areas: pool-riffle, plane-bed, step-pool, cascade and colluvial with the steepest morphology. These different morphologies exhibit different productivities for salmonids and other aspects of the aquatic ecosystem in these mountain watersheds.

The volcanic watershed has the least amount of pool-riffle sections of all three study areas with only about 2 % of the whole drainage basin. On the other side the basin features with 40% of cascade sections the highest amount of all other lithologies (figs. 12-14).

The Sedimentary basin has the highest amount of 42% plane-bed-, and 12% step-pool sections of all lithologies but displays only 4% of steeper colluvial areas.

The Granitic basin shows with 15% of pool-riffle sections and 11% of colluvial sections the lowest elevations with flatter river systems but also the steepest colluvial slopes within the stream networks of the three watersheds (figs. 12-14).

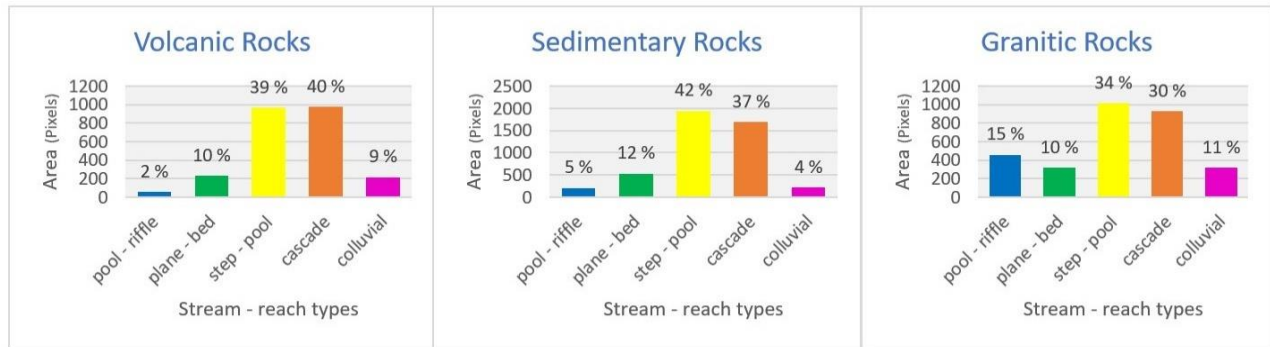


Figure 12: Statistical distribution of all stream-reach types in percentage of the whole area in all three lithological watersheds.

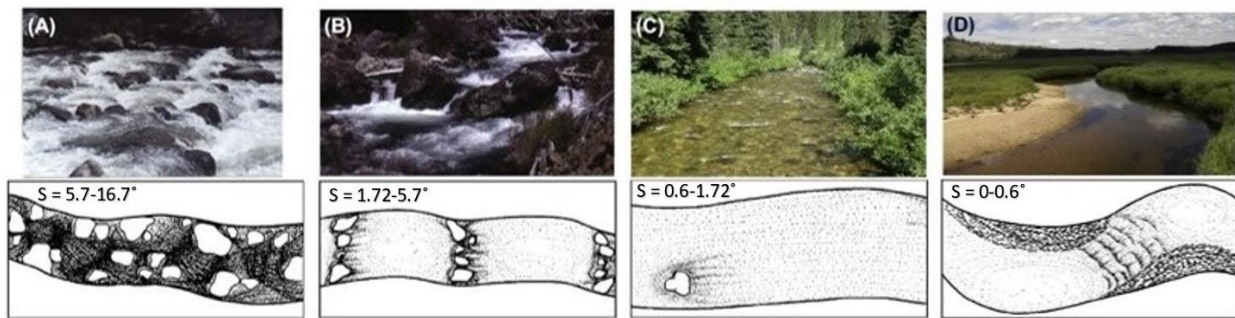


Figure 13: Photographs and plan-view sketches of the alluvial stream types. (A) cascade, (B) step-pool, (C) plane-bed, (D) pool-riffle. (After Bisson et al., 2017 and Montgomery and Buffington, 1997)

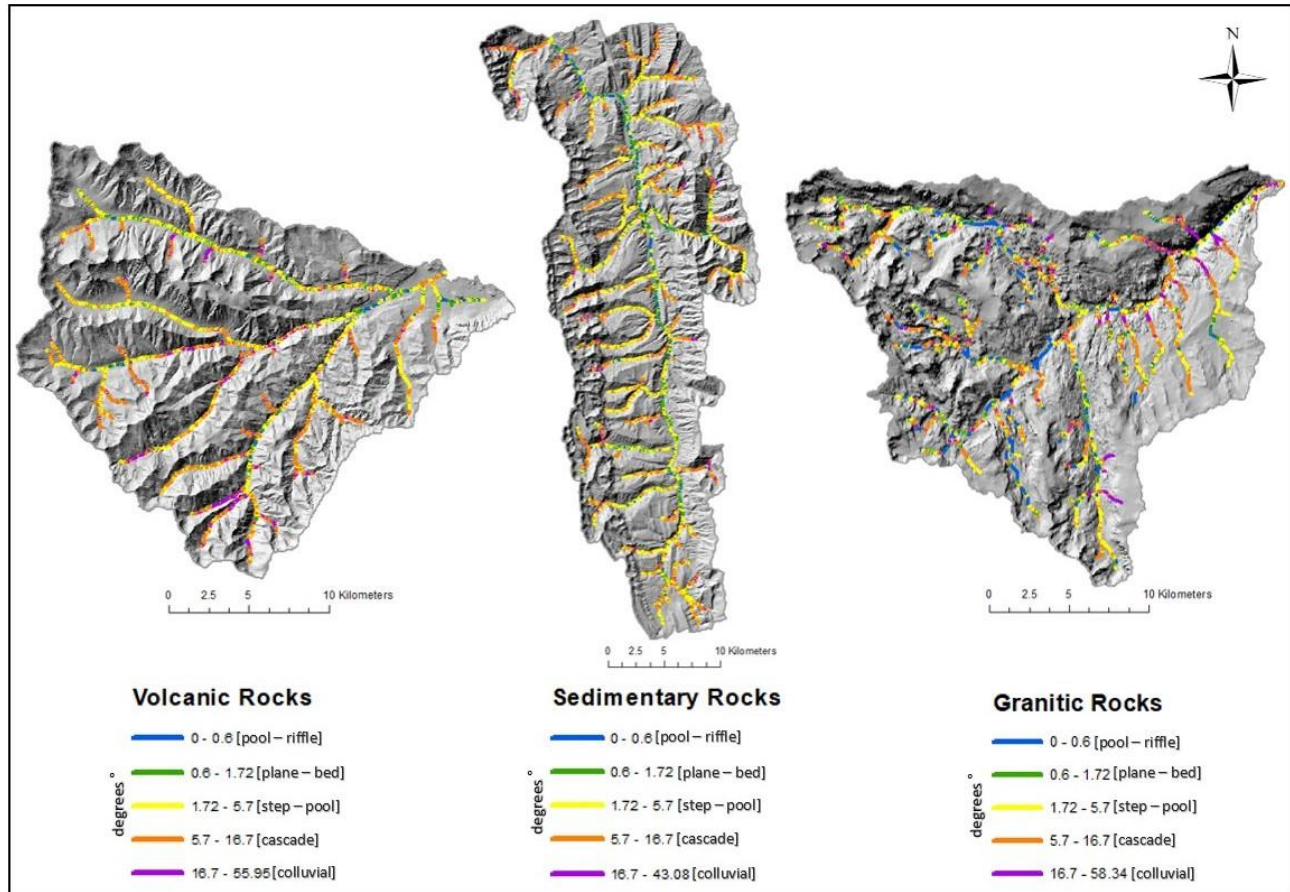


Figure 14: Reclassification of the topographic steepness gradient in the drainage network after Montgomery and Buffington.

6. Discussion

The morphometric analyses of the three drainage areas showed significant differences in their valley shapes and longitudinal profiles. First, the resistant granite especially differed from the volcanic and sedimentary basins with its stair-stepped longitudinal profile, while the other two basins were shaped much smoother because of their less resistant bedrock. Second, because glacial erosion has played such a major role in the recent development of valley profiles, morphological adjustment of streams and rivers in the post-glacial valleys is also strongly controlled by the different patterns of glacial erosion.

6.1. Glacial valley morphology related to rock strength and lithology

Bedrock strength characteristics are an important factor in controlling the morphology of glacial valleys (Brook et al., 2004). For example, they found that glaciers in closely jointed metasedimentary bedrock with low rock mass strength developed broad U-shaped valleys, whereas igneous bedrock with a high rock mass strength developed steeper sided, narrower cross valleys.

Even though in this study no rock mass strength was measured in the field, the results support this theory (fig. 9). Hence it is important to take a closer look at the involved processes of how glaciers formed those valleys. According to Benn and Evans (1998) abrasion and quarrying are the main driving forces for glacial erosion of hard rock beds. Those two processes are delineated by Anderson and Anderson (2010) as follows. Subglacial abrasion is erosion resulting from the sum of all scratches, which are products of individual rocks that were embedded in the sole of the glacial ice as it slid across the bedrock. The theory behind this was worked out by Bernard Hallet (1979) following the equation $e = C \cdot A_s \cdot U_c$. The abrasion rate $[e]$ is the concentration of fragments per unit area of bed $[C]$, $[A_s]$ is the area of the indentation that they induce in the bedrock, and $[U_c]$ is the rate at which the striators are dragged across the rock (fragment velocity). Anderson and Anderson (2010) describe quarrying as a process where beds with larger bumps are causing subglacial cavities on the lee sides and as the ice is flowing over the top of those bumps, they are then getting separated from the bed in the lee and as a result, all but those subglacial cavities at the edges of the glacier will be filled with water (Anderson and Anderson, 2010). This mechanism also involves the generation of cracks in the bedrock

at the edge of a cavity, and results from imbalance of forces on the top and sides of the rock bump (Anderson and Anderson, 2010).

Hence because both the sliding speed, which dictates the abrasion rate, and the water-pressure fluctuation, which strongly modulates the quarrying rate, should peak at the equilibrium-line altitude (ELA), and most rapid erosion should follow the transient ELA (MacGregor et al., 2000). The ELA separates the accumulation zone above from the ablation zone below (Anderson et al., 2006). The ELA has moved up and down valley as the glacier grows and recedes – in this process the sedimentary and volcanic profiles were smoothed. On the other hand, the glacial erosion is maximized where the ice gains thickness from tributaries – so small tributaries stay perched and the valley is more stair-stepped.

Furthermore Harbor (1995) expounds that erosion dominates towards the base of valley sidewalls, generating U-shaped valleys that are also clearly visible in my results. The granite basin with the resistant bedrock shows steeper sided slopes, whereas the volcanic and sedimentary basins developed broader and flatter glacial valleys, reflecting the importance of bedrock strength on glacial erosional development of the landscape (Brooks et al., 2016).

Another important point is that if glaciers have simply exploited a pre-existing valley system, in which the troughs are deep and narrow, then the final valley shapes may simply be reflecting this earlier influence rather than having the shape controlled by their rock mass strength. Thus, glaciers flowing in deep narrow valleys also produce deep narrow valleys after deglaciation. Certainly, pre-existing valleys are a big factor in constraining the flow of glaciers, and hence are an influence on the final through cross-profile form

(Augustinus, 1991). The rivers in this study all have similar topographic relief and drainage areas, but differences in tectonic history or lithology would have also affected the river profile development prior to glaciation.

MacGregor et al. (2000) suggests that glaciated valleys can be easily identified by the characteristics of their longitudinal profiles that contrast strongly with fluvial valley forms. Although longitudinal river profiles are also smooth and decrease in slope downvalley, glaciated valleys have wide, low-gradient floors punctuated by multiple steps and overdeepenings tens to hundreds of meters deep (MacGregor et al., 2000). These distinctive glacial signatures are the result of thousands of years of erosion. The steps or overdeepenings in glaciated valleys, very nicely shown in the granitic profile (fig. 9), may result from variation in glacier length over multiple climate cycles. Alley et al. (1999) and Hooke (1991) claim that high basal water pressure in existing overdeepenings can localize subglacial erosion. Further, Nye and Martin (1967) maintain that the ice flow field, which is in some cases associated with tributary junctions, may also be responsible for enhanced local erosion. Thus, the enhancement of glacial erosion below tributary junctions may be expected due to increase in ice mass and thickness.

Another important characteristic for such systems is that the ice discharge is a proxy for the long timescale pattern of erosion that stamps the glacial fingerprint over the fluvial morphology. Present- and paleo glaciers that are reconstructed from moraine patterns normally have more than half of their surface area at elevations above the ELA. This also reflects the hypsometry of the glaciated basin and the dependence of local mass balance (accumulation minus melt) on altitude. Longitudinal profiles are commonly steepened in their headwaters and reduced to lower slopes in the reaches near the

terminal moraines that mark the glacial limit. Also, glacial long-valley profiles often show significant steps not seen in fluvial valleys and while some steps clearly coincide with variations in rock resistance, the most prominent steps in the profile often concur with tributary junctions. Where headwaters valleys coalesce, the character of the valley floor usually changes from a knobby, disorganized surface to a smooth U-shaped conduit down valley. Penck (1905) was the first one who emphasized that river discharge monotonically increases downstream as it gathers water from hillslopes and tributaries and therefore a rivers ability to erode rock is most often assumed to depend upon both water discharge and slope of the bed. Hence, as the water discharge increases downstream, the slope required for incision of rock declines which results in the smooth concave-up longitudinal profile characteristic of fluvial valleys.

6.2. Valley stream morphology based on stream-reach types

The best solution to get a good visualization of the stream network in all three drainage basins was a classification of different stream-reach types in those watersheds (fig.13). Reach morphology in alluvial valleys is first related to characteristics of sediment supply like grain size and rate of input, second to the power of the stream to mobilize its bed (a function of stream flow and topographic gradient) and third the degree of channel confinement by valley walls (Bisson et al., 2017). Here I classify the stream reaches based on stream gradient using the classification of Montgomery and Buffington (1997), where the individual stream types reflect the factors above (fig.12).

6.2.1. Colluvial Valleys

The steepest parts of the drainage basins are referred as colluvial which serve as temporary repositories for sediment and organic matter eroded from surrounded hillslopes. In such valleys fluvial transport is relatively ineffective at removing materials deposited on the valley floor because sediment and organic matter moderately accumulate in headwater valleys until periodically flushed by debris flows in steep terrain. After the removal of the accumulated sediment by large disturbances, the colluvial valleys begin refilling again (Dietrich et al., 1986). Thus, there can be differentiated between unchanneled and channeled colluvial valleys where first are headwater valley segments with lacking recognizable stream channels and latter contain low-order stream immediately downslope from the unchanneled colluvial valleys, commonly forming the upper part of the stream network. In general, the flow in colluvial channels tend to be shallow and transient due to the small drainage areas that are not supporting the sustained stream flow. In alpine areas, colluvial channels may scour to bare bedrock.

6.2.2. Alluvial Valleys

According to Bison et al. (2017) alluvial valleys are another subdivision type of valley segments which are supplied with sediment from upstream sources and adjacent hillslopes. Thus, the sediment transport capacity of an alluvial valley is insufficient to scour the valley floor to bedrock. As a result, the valley fill accumulates primarily of fluvial origins. Further alluvial valleys are in many landscapes the most common type of valley segment and can be classified in different stream-reach types. In this study the focus was on Cascade-, step-pool-, plane-bed-, and pool-riffle reaches.

6.2.2.1. Cascade

The cascade reaches are the steepest alluvial channels with steepness gradients ranging from 5.7 to 16.7 degrees, occurring typically in headwater areas that are strongly confined by valley walls and have therefore a small width-to-depth ratio. There may be a few small turbulent pools present in those reaches, though most of the flowing water is tumbling over and around closely spaced boulders or larger wood. Those boulders are supplied from adjacent hillslopes or from periodic debris flow depositions (Bisson et al., 2017).

6.2.2.2. Step-pools

The step-pool reaches possess boulders and logs with discrete channel-spanning accumulations that are forming a series of vertical steps alternating with pools containing finer substrata and their capacity temporarily store fine sediment and organic matter that generally exceeds that of cascade reaches. Most of those channels tend to be relatively straight with steepness gradients of 1.72 to 5.7 degrees. Further, they comprise coarse but heterogenous substrata (gravel to boulders), with small width-to-depth ratios and moderate confinement by valley walls (Montgomery and Buffington, 1997; Bison et al., 2017)

6.2.2.3. Plane-beds

The plane-bed reaches are characterized by long, relatively straight channels of uniform depth that typically have moderate slopes with 0.6 to 1.72 degrees and their streambeds are predominantly composed out of gravel and cobble. Hence, they usually exhibit intermediate values of stream gradients, width-to depth ratio, and relative submergence (the ratio of flow depth to median particle size. Moreover plane-bed reaches

also can show more extensive floodplain development than step-pool and cascade reaches (Montgomery and Buffington, 1997; Bison et al., 2017).

6.2.2.4. Pool-riffles

Pool-riffle reaches are prevalent in alluvial valleys of low-to- moderate gradients with 0 to 0.6 degrees and are commonly associated with small to mid-sized streams. They are frequently sinuous and are characterized for an undulating streambed that is formed by pools, riffles and bars. Pools are topographic depressions in the stream bottom that is caused by local flow convergence and scour. Otherwise, bars are complimentary areas of flow divergence and deposition, forming the highest points of the channel. Riffles are located at crossover areas from pools to bars and at low streamflow, the water meanders around bars and through pools and riffles that are commonly alternating from one riverside to the other (Montgomery and Buffington, 1997; Bison et al., 2017).

In general, there are both more colluvial-, but also more pool-riffle reaches in the granitic basins with the stepped profile. The smoother shaped volcanic and sedimentary watersheds contrary display less pool-riffles but boths show a higher frequency of step-pool reaches and also cascade reaches, whereas the volcanic basin features the highest amount of them. Because post-glacial incision of streams is probably only several meters at most, post-glacial mountain stream diversity is a function of the glacial history. Importantly, the interactions of glaciers with geology thus shapes the drainage network that is utilized by the modern ecosystem and by humans for water development and recreation.

7. Conclusion

The three watersheds in north-western Wyoming feature contrasting landscapes and valley shapes: the volcanic basin in the Absaroka Range shows a quite smooth profile with few steps in higher elevations that are almost not visible, whereas the sedimentary valley depicts a completely smooth longitudinal profile. However, the granitic catchment area shows a stepped profile which is characteristic for resistant bedrock. Those results suggest that the glacial erosion was most effective in the sedimentary basin followed by the volcanic watershed, which shows similar characteristics but retains higher relief. By contrast, the granitic basin illustrates the impacts of the resistant bedrock during glacial valley erosion with the steep valley walls, but also the low gradient sections of tributary valleys at some of the highest elevations, which represent hanging valleys and cirques that are much rarer in the Absaroka and Wyoming Ranges. Additionally, the granitic basin shows less deep valley incision compared to the volcanic and sedimentary basins with deep river valleys and isolated peaks.

The stream-reach types in the different drainage basins display the supposed high colluvial frequency in the granitic basin, whereas the sedimentary watershed shows the least. Yet the granitic basin also had the most low-gradient pool-riffle streams because of abundant low-gradient stream sections between steps in the profile. Thus, the drainage systems are strongly affected by the erosional processes of the glacially formed valleys.

8. References

- Anderson, R.S., Riihimaki, C.A., Safran, E.B. and MacGregor, K.R., 2006. Facing reality: Late Cenozoic evolution of smooth peaks, glacially ornamented valleys, and deep river gorges of Colorado's Front Range. Geological Society of America Special Paper 398, p.397.
- Burrough, P. A., and McDonell, R. A., 1998. Principles of Geographical Information Systems (Oxford University Press, New York), 190 pp.
- Frost, B.R., Chamberlain, K.R., Swapp, S., Frost, C.D. and Hulsebosch, T.P., 2000. Late Archean structural and metamorphic history of the Wind River Range: Evidence for a long-lived active margin on the Archean Wyoming craton. Geological Society of America Bulletin, 112(4), pp.564-578.
- Horton, J.D., San Juan, C.A., and Stoesser, D.B., 2017, The State Geologic Map Compilation (SGMC) geodatabase of the conterminous United States (ver. 1.1, August 2017): U.S. Geological Survey Data Series 1052, 46 p., <https://doi.org/10.3133/ds1052>.
- MacGregor, K.R., Anderson, R.S., Anderson, S.P. and Waddington, E.D., 2000. Numerical simulations of glacial-valley longitudinal profile evolution. Geology, 28(11), pp.1031-1034.
- Sugarbaker, L.J., Eldridge, D.F., Jason, A.L., Lukas, Vicki, Saghy, D.L., Stoker, J.M., and Thunen, D.R., 2017, Status of the 3D Elevation Program, 2015: U.S. Geological Survey Open-File Report 2016–1196, 13 p., <http://dx.doi.org/10.3133/ofr20161196>.
- Tarboton, D. G., R. L. Bras, and I. Rodriguez–Iturbe. 1991. "On the Extraction of Channel Networks from Digital Elevation Data." Hydrological Processes 5: 81–100.
- Strahler, A.N. (1957) Quantitative analysis of watershed geomorphology. Transactions of the American Geophysical Union, 38, 912–920.

Pierce, K.L., 2003. Pleistocene glaciations of the Rocky Mountains. *Developments in Quaternary Sciences*, 1, pp.63-76.